Available online at www.sciencedirect.com

SciVerse ScienceDirect

Ceramics International 39 (2013) 977–982

CERAMICS INTERNATIONAL

www.elsevier.com/locate/ceramint

Microstructure and mechanical properties of Al_2O_3–20 wt%Al_2TiO_5 composite prepared from alumina and titania nanopowders

Sh. Mohseni Meybodi[a], H. Barzegar Bafrooei[b,*], T. Ebadzadeh[b], M. Tazike[b]

[a]*Islamic Azad University, Maybod Branch, Maybod, Iran*
[b]*Ceramic Division, Materials and Energy Research Center, P.O. Box 14155-4777, Tehran, Iran*

Received 7 July 2011; received in revised form 20 June 2012; accepted 4 July 2012
Available online 20 July 2012

Abstract

In the present work, Al_2O_3–20 wt%Al_2TiO_5 composite was prepared from reaction sintering of alumina and titania nanopowders. The nano-sized raw powders were reconstituted into nanostructured particles by ball milling. Then, the nanostructured reconstituted powders were pressed and pressureless-sintered into bulk ceramics at 1300, 1400, 1500 °C for 2 h. The phase composition and microstructures of reconstituted powders and as-prepared ceramic composites were characterized by using X-ray diffractometer (XRD), scanning electron microscope (SEM), transmission electron microscope and energy-dispersive spectrometer (EDS). The microstructural analysis of the ceramic showed that the average grain size of the alumina–aluminium titanate composite increases with increasing the temperature. Also, SEM proved the existence of a proper interface between Al_2TiO_5 and Al_2O_3 grains and preferential distribution of aluminium titanate particles in the grain boundaries. XRD analysis indicated the absence of rutile titania in the sintered composite ensuring complete formation of aluminium titanate. The hardness of the samples sintered at 1300, 1400, 1500 °C were 4.8, 6.2 and 8.5 GPa, respectively.

Keywords: C. Mechanical properties; Alumina; Aluminium titanate; Nanostructure composite powders

1. Introduction

Aluminium titanate (AT), Al_2TiO_5, is known to be a promising candidate material in refractory and engine components because of its low thermal expansion, excellent thermal shock resistance, and low thermal conductivity [1]. AT exhibits two allotropic forms: α and β, where β-AT is the stable phase [2]. In general, AT can be formed by the solid-state reaction between Al_2O_3 and TiO_2 above the eutectoid temperature of 1280 °C [3]. AT exhibits microcracking during cooling from the sintering temperature especially above the critical sintered grain size of 1.5 μm. This fact will bring about the necessity for obtaining fine-grained microstructures [4]. Alumina is widely employed in various applications because of its high thermal stability, chemical inertness and wear resistance [5]. In alumina based composites, much attention has been focused on the improvement of fracture toughness and thermal shock resistant in alumina either by the addition of second phase or by the microstructure designs such as duplex [6] or duplex-bimodal [7], heterogeneous [8–10], and layer structures [11–13]. Earlier reports suggest the addition of AT particles of controlled size to improve the thermo-mechanical response of alumina–AT composite [14–16]. Improved flaw tolerance has been observed as a result of the addition of AT due to induced residual stresses by virtue of thermal expansion mismatch between alumina and AT [7]. The functional and structural properties of alumina–AT composite has made them suitable choices for applications such as thermal barrier coatings, insulating components for diesel engines and high temperature substrates. Further improvement in mechanical properties of alumina–AT composite is attributed to the combined

*Corresponding author. Tel.: +98 263 6204130; fax: +98 263 6280030.
E-mail address: hadi.merc@gmail.com (H. Barzegar Bafrooei).

0272-8842/$ - see front matter © 2012 Elsevier Ltd and Techna Group S.r.l. All rights reserved.
http://dx.doi.org/10.1016/j.ceramint.2012.07.015

effect of internal stresses developed due to AT and large particle size of alumina [17]. Nieto et al. [18] reported on the reaction sintering of colloidal mixtures using sub-micrometric alumina and nano-titania. Jayasankar et al. [14] studied the role of particle size of alumina on the formation of aluminium titanate as well as the sintering and microstructural development in sol–gel alumina–aluminium titanate composites. In the present study, The effect of nanostructure powder mixture and sintering temperature on the microstructural development and mechanical properties of alumina–AT composite through a reaction sintering method has been investigated.

2. Experimental

Al_2O_3 (α phase, 99% grade, PL-A-AlO, Plasma chem, Germany) and TiO_2 (mixture of anatase and rutile, 99% grade, P25, Degussa Co., Frankfurt, Germany) nanopowders were used as the received powders. The nanosized powders were blended in a ball-mill uniformly to produce a powder mixture containing 80 wt% Al_2O_3 and 20 wt% TiO_2. Powder mixtures were uniaxially compacted under different loads in a rigid die (10 mm diameter) using PVA as the binder. The green density was obtained by measuring the ratios of weight to volume of the green compacts. These compacts were sintered at temperatures of 1300, 1400 and 1500 °C for 2 h in air. In order to obstruct the decomposition of aluminium titanate, a cooling rate of 30 °C/min in the temperature range of 1200–800 °C was applied. An X-ray diffraction instrument with CuKα radiation (Philips, X'Pert) was used to determine the phase composition. Microstructural observations were performed using a scanning electron microscope (Philips XL30, Netherlands) equipped with energy dispersive X-ray spectrometer (EDS). Transmission electron microscope (TEM, CM200FEG, Philips, Netherlands) was employed to determine the size and shape of the nanoparticles. Mechanical properties were assessed by Vickers micro-indentation using loading values of about 9.8–98 N (from 1 to 10 kg). Ten indents were made for each measurement and hardness was calculated using Eq. (1) according to ASTM C1327 [19].

$$H = 1.854(P/d^2) \quad (1)$$

where 'H' is the hardness, 'P' is the indentation load, 'E' is the elastic modulus (assumed to be 390 GPa), 'K_c' is the indentation toughness, and 'd' and 'c' are the indent diagonal length and the crack length, respectively. The density of the sintered specimens was measured by the Archimedes method using distilled water as the liquid.

3. Results and discussion

The morphology (TEM micrographs) and XRD pattern of the TiO_2 nanopowder are shown in Fig. 1. TEM microscopy reveals a particle size of 11–27 nm for TiO_2 nanoparticles. The phase content of the as-received powder was calculated

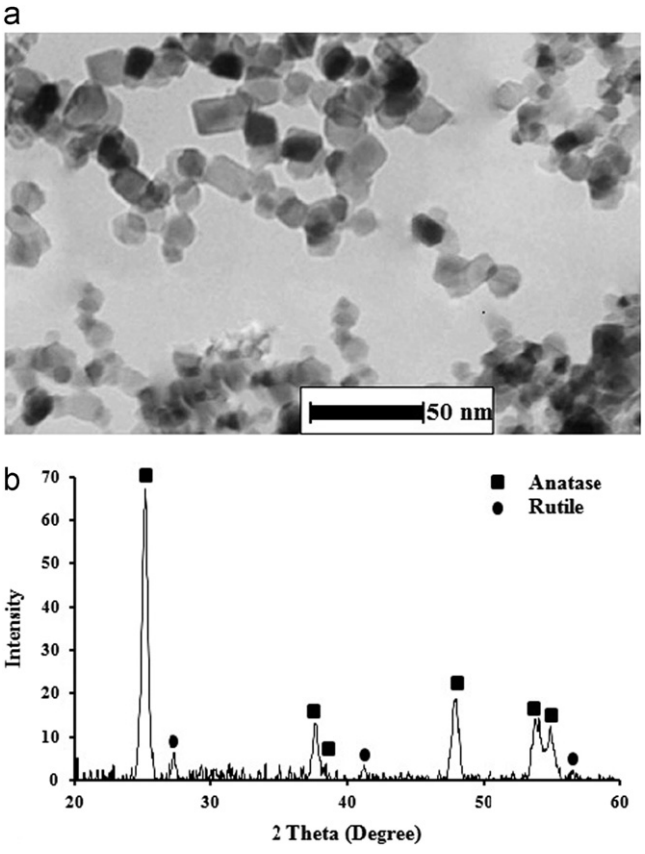

Fig. 1. (a) Transmission electron microscopy (TEM) micrograph and (b) X-ray diffraction (XRD) pattern of as-received TiO_2 nanopowder.

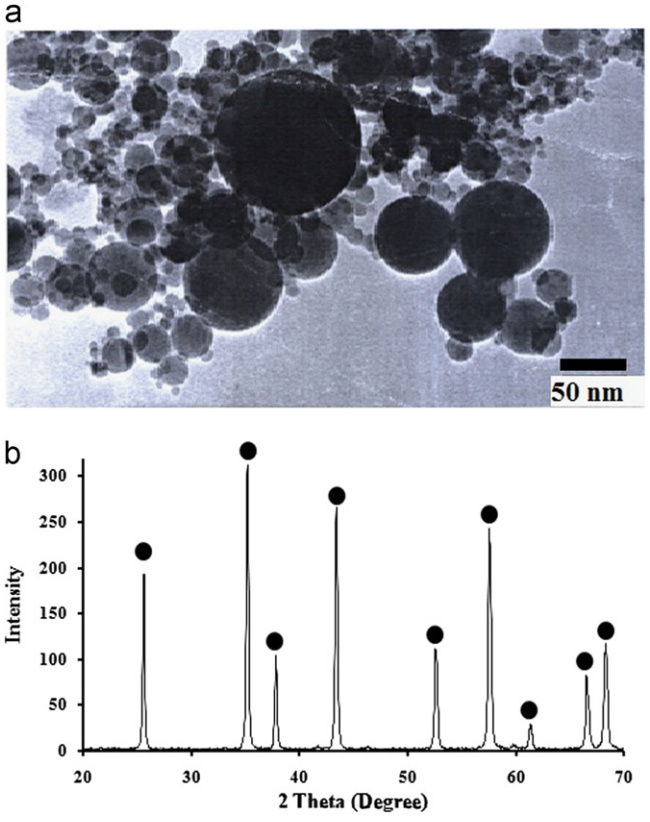

Fig. 2. (a) Transmission electron microscopy (TEM) micrograph and (b) X-ray diffraction (XRD) pattern of as-received Al_2O_3 nanopowder.

from XRD pattern (Fig. 2b) to distinguish anatase and rutile phases via their peak intensities (described in detail springer [20]). The fraction of anatase and rutile phases within the starting powder was found to be 77% and 23%, respectively. The crystallite size of the anatase and rutile phases was determined to be 21.7 and 14.5 nm, respectively, based on the Scherrer equation. TEM and XRD results showed that the particle size of alumina nanopowder is in the range of 5–150 nm with phase composition of α-Al_2O_3 (Fig. 2a and b). Fig. 3a and b shows the morphology and XRD pattern of the reconstituted powders, respectively. It can be observed that the nanostructured reconstituted powders consist of agglomerates composed of fine crystallites powder (Fig. 3a). Fig. 3b shows the XRD patterns of the nanostructured reconstituted powders. The mixture shows mainly three major crystalline phases: α-Alumina, rutile and anatase which are similar in phase composition to the nanosized raw powders. Powder compressibility is considered as one of the most crucial factors in producing dense ceramics directly affecting the compact green density and consequently the fired density of the final product. The compaction mechanism of brittle powders in a rigid die is typically considered in three stages including: (I) sliding and rearrangement of the particles; (II) fragmentation of brittle solids and (III) elastic deformation of bulk compacted powders [21]. In the first

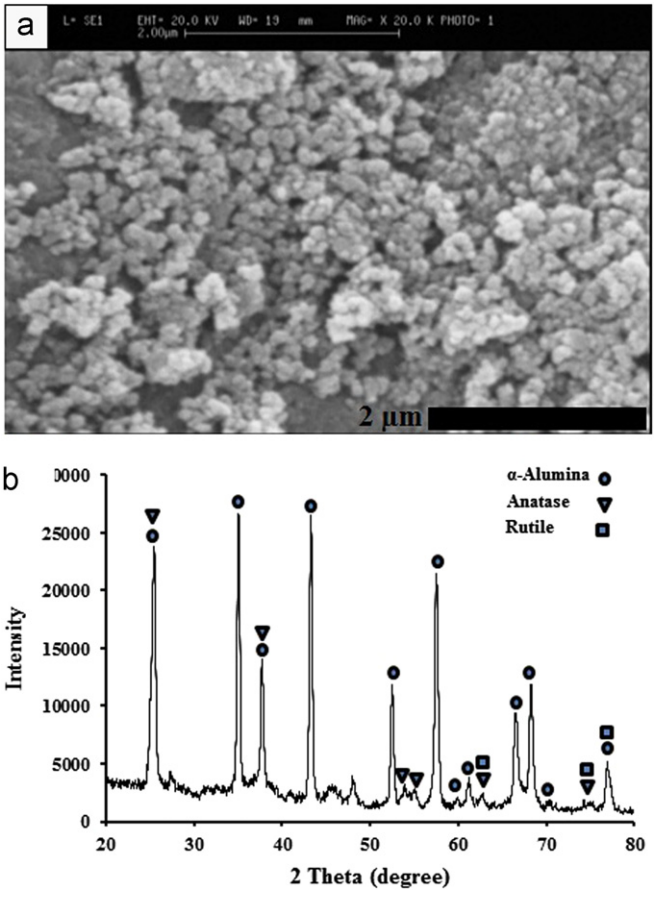

Fig. 3. (a) Scanning electron microscopy (SEM) micrograph and (b) X-ray diffraction (XRD) pattern of Al_2O_3–TiO_2 nanocomposite powder.

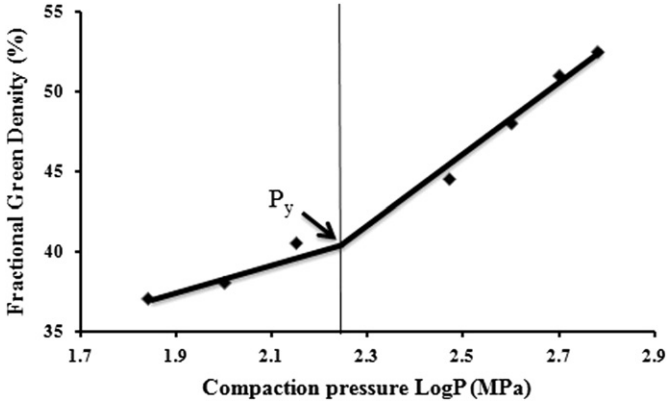

Fig. 4. Fractional green densities of composite nanopowder as function of log compaction pressure (P).

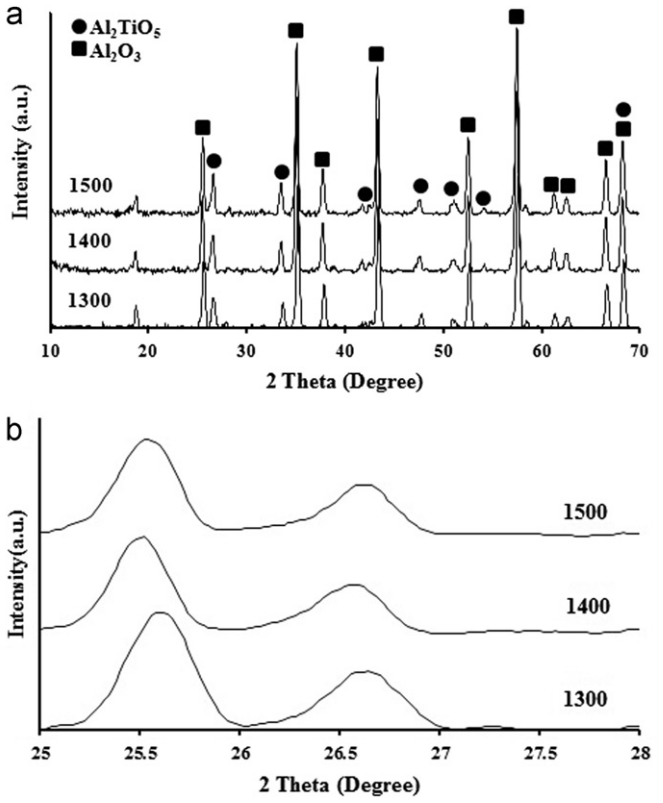

Fig. 5. (a) XRD patterns of the composites obtained from the nanostructured Al_2O_3–TiO_2 powders sintered at different sintering temperatures (b).

Table 1
Properties of Al_2O_3–20 wt% Al_2TiO_5 ceramic composites obtained at different sintering temperatures.

Sintering temperature (°C)	Relative density (%)	Apparent density (g/cm^3)	Vickers hardness (GPa)
1300	87.3	3.41	4.8 ± 0.3
1400	91.05	3.55	6.2 ± 0.5
1500	94.1	3.67	8.5 ± 0.7

stage of the compaction process, particle sliding and rearrangement of the agglomerated particles are the dominant mechanisms of consolidation. When the applied pressure increases, the movement of the particles is restricted and the energy applied to the powder compact is generally spent through the fragmentation process of agglomerates and friction losses. Zevert et al. [22] showed that in the case of

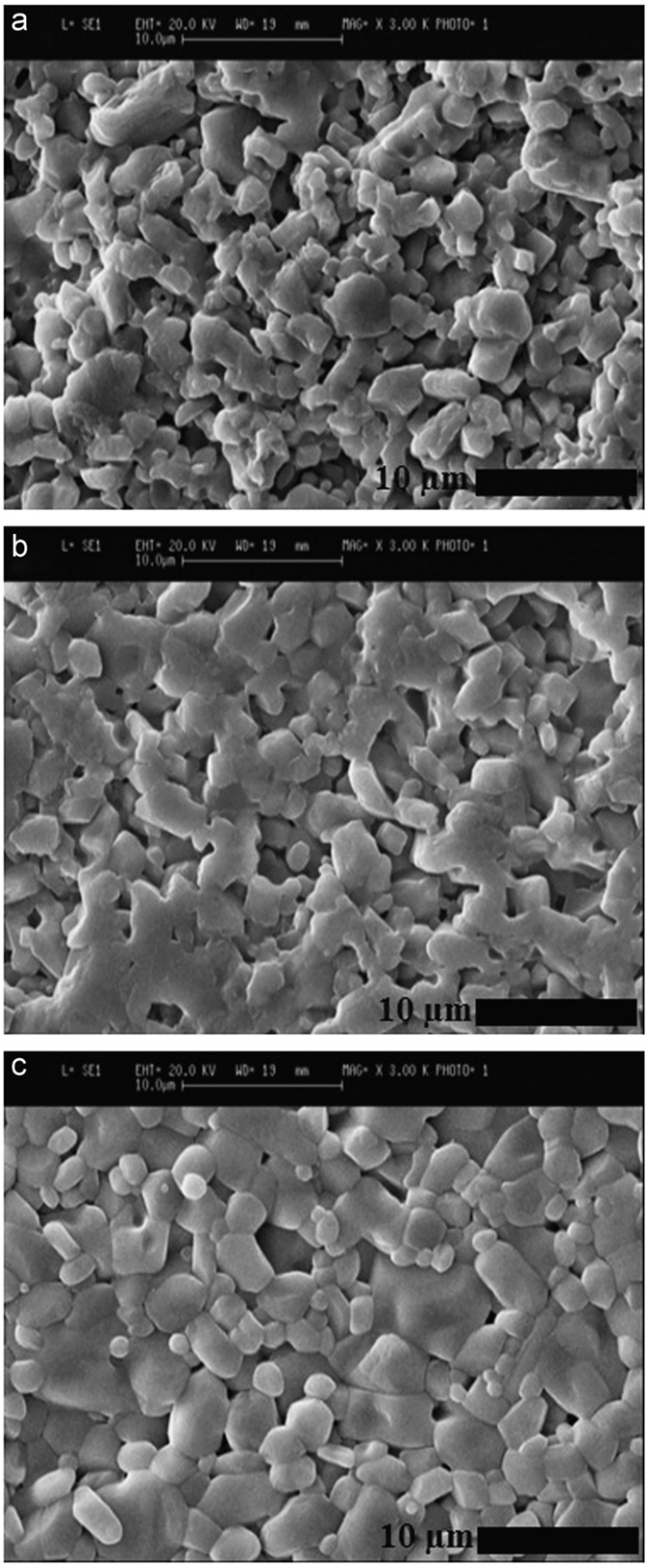

Fig. 6. SEM micrographs of nanostructured Al_2O_3–20 wt% TiO_2 powders sintered at different sintering temperatures for 2 h ((a–c) corresponding to 1300 °C, 1400 °C, 1500 °C).

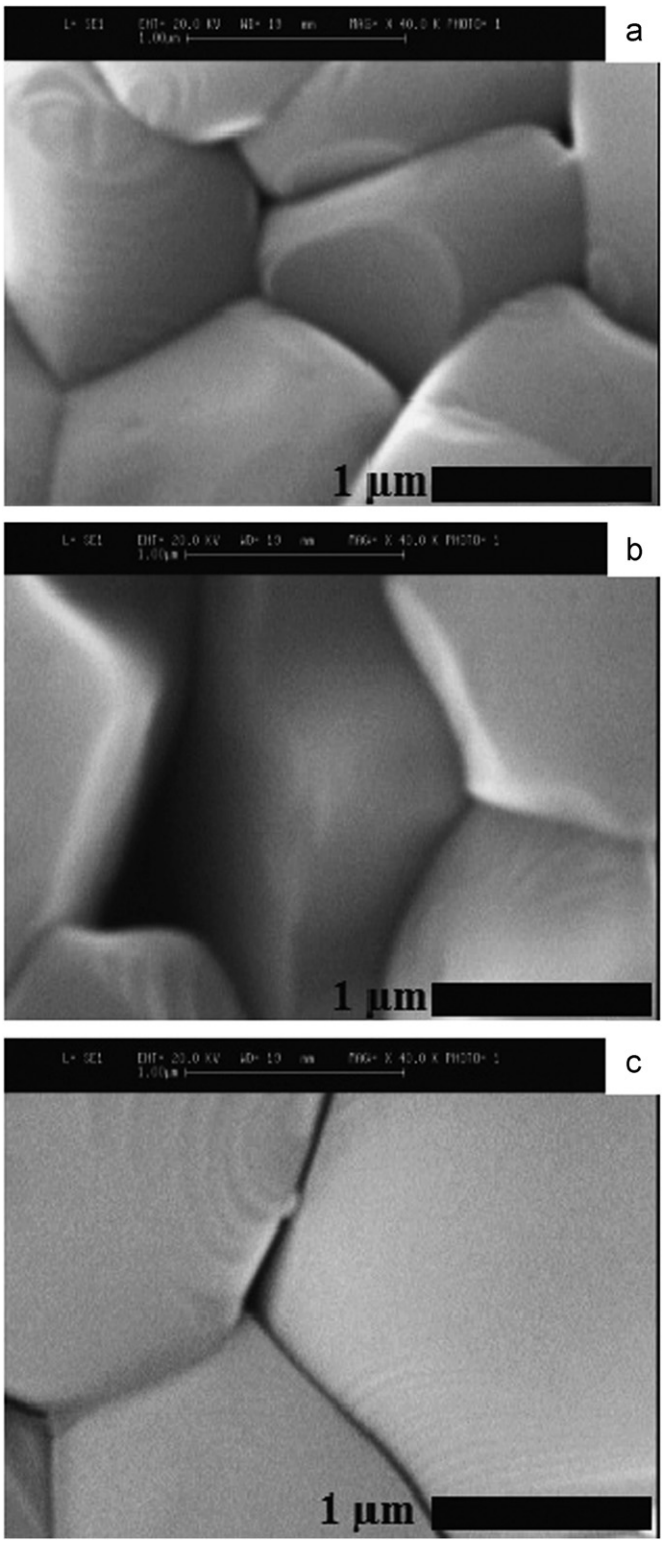

Fig. 7. High magnification SEM micrographs of nanostructured Al_2O_3–20 wt% TiO_2 powders sintered at different sintering temperatures for 2 h ((a–c) corresponding to 1300 °C, 1400 °C, 1500 °C).

the agglomerated powders, there was a turning point (P_y) in the plot of the relative density versus the logarithm of the applied pressure as shown in Fig. 4. The curve was divided into two sharply separated linear parts with an interception at point P_y which is called the "strength of the agglomerates". After compaction at a pressure around P_y, these agglomerates are gradually fragmented and then rearranged at lower pressures [22]. In this case, the agglomeration strength of the powder is about 156 MPa. The value of P_y depends heavily on the synthesis method and calcination temperature [23] (Fig. 4).

Fig. 5a and b illustrates the X-ray diffraction patterns recorded from the Al_2O_3–20 wt% AT composite sintered at different temperatures for 2 h. The XRD results clearly indicate that the composites sintered at different temperatures are composed of the same phases, i.e. α-Al_2O_3 and AT. The latter is formed during the reaction sintering of Al_2O_3 and TiO_2. The absence of diffraction peaks in the XRD patterns of TiO_2 is attributed to the reaction of TiO_2 and Al_2O_3 to form AT. To better compare the relative intensities of alumina and aluminium titanate composite, The XRD pattern of sintered microstructures were applied in the 2θ range between 25 and 28. These results confirm that aluminium titanate is obtained through the reaction sintering of alumina and titania nanopowder at temperatures between 1300 and 1500 °C according to previous results for micron-sized materials [14,17,18]. The density and mechanical properties of Al_2O_3–20 wt% AT bulk composites sintered at different temperatures are listed in Table 1. As the sintering temperature increased from 1300 to 1500 °C, The apparent and relative densities increased from 3.41 to 3.67 g/cm^3 and 87.3 to 94.1%, respectively. This can be attributed to a large number of contact points formed because of the nanostructured composite powders and the higher fraction of fine particles resulting in shorter diffusion paths. In such conditions, the average coordination number

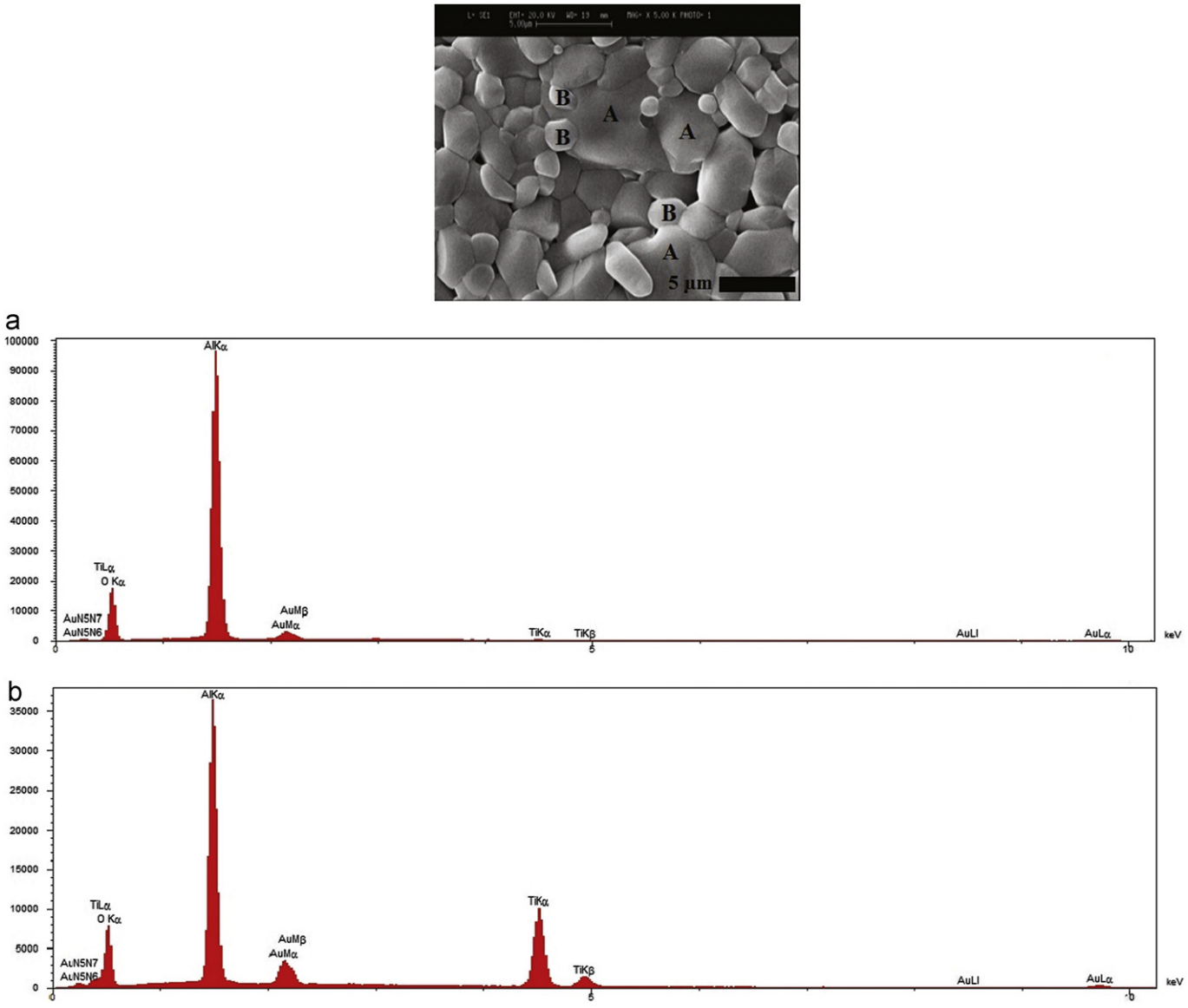

Fig. 8. Nanostructured Al_2O_3–20 wt% TiO_2 powders sintered at 1500 °C (marked area is the spot where the EDX analysis was performed).

of particles will be increased leading to enhanced sintering [24]. In spite of using nanosized raw powders, considerable increase in the relative density of the sintered samples could probably be ascribed to the agglomeration of nanosized raw materials powder particles. The mechanical properties of the reaction sintered Al_2O_3–20 wt% AT ceramics are also shown in Table 1. From this table, the relationship between Vickers hardness showed the same trend as the one between relative density and sintering temperature. As known, ceramics prepared by the nanostructured powders obtain highly homogeneous microstructure as a result of their enhanced sintering behaviour than those prepared by micron size powders. Therefore, the nanostructured composites have more improved mechanical properties compared with the microstructured composites. reported in literatures. The microstructure of the polished surfaces of Al_2O_3–20 wt%AT sintered at different temperatures is shown in Fig. 6. Addition of AT to Al_2O_3 is expected to control the grain growth of both alumina and aluminium titanate. No microcracking is observed in any of the samples sintered at different temperatures indicating the absence of abnormal growth of AT grains. Under present preparation conditions, the aluminium titanate particles are preferentially distributed at grain boundaries which could be a result of the nanostructured composite powder as well as the homogenous distribution of alumina and titania nanopowders. Also, high magnification SEM revealed a proper interface between AT and Al_2O_3 grains along with preferential distribution of aluminium titanate particles in the grain boundaries Fig. 7. The distribution of aluminium titanate grains in the alumina matrix was confirmed by SEM–EDX analysis as shown in Fig. 8. The microstructural analysis of the composite sintered at 1500 °C shows that the grain size of aluminium titanate is lower than that of alumina (Figs. 7 and 8).

4. Conclusion

Al_2O_3–20 wt% AT composites were prepared by the reaction sintering of alumina and titania nanopowders at different temperatures. The relative density of the composite after sintering at 1500 °C was 94.1%. No further increase in density was detected which is attributed to agglomeration of particles within the initial mixture. The XRD pattern analysis confirmed the formation of aluminium titanate in the Al_2O_3–20 wt% composite sintered at 1300–1500 °C. Elevated sintering temperatures also improved the hardness to 8.5 GPa.

References

[1] H.A.J. Thomas, R. Stevens, Aluminum titanate a literature review, Part 1: microcracking phenomena, British Ceramic Transactions and Journal 88 (1989) 144–151.
[2] A.V. Prasadarao, U. Selvaraj, S. Komarneni, A.S. Bhalla, R. Roy, Enhanced densification by seeding of sol–gel-derived aluminum titanate, Journal of the American Ceramic Society 75 (1992) 1529–1533.
[3] E. Kato, K. Daimon, J. Takahashi, Decomposition temperature of B-Al_2TiO_5, Journal of the American Ceramic Society 63 (1980) 355–356.
[4] N.P. Padture, J.L. Runyan, S.J. Bennison, L.M. Braun, B.R. Lawn, Model for toughness curves in two-phase ceramics, II: microstructural variables, Journal of the American Ceramic Society 76 (1993) 2241–2247.
[5] J.L. Runyan, S.J. Bennison, Fabrication of flaw-tolerant aluminum titanate-reinforced alumina, Journal of the European Ceramic Society 7 (1991) 93–99.
[6] M.P. Harmer, H.M. Chan, G.A. Miller, Unique opportunities for microstructural engineering with duplex and laminar ceramic composites, Journal of the American Ceramic Society 75 (1992) 1715–1728.
[7] N.P. Padture, S.J. Bennison, H.M. Chan, Flaw-tolerance and crack-resistance properties of alumina–aluminum titanate composites with tailored microstructures, Journal of the American Ceramic Society 76 (1993) 2312–2320.
[8] P.L. Chen, I.W. Chen, In-situ alumina/aluminate platelet composites, Journal of the American Ceramic Society 75 (9) (1992) 2610–2612.
[9] J. Wang, C.B. Ponton, P.M. Marquis, Silver-toughened alumina ceramics, British Ceramic Transactions 92 (2) (1993) 67–74.
[10] L. An, H.M. Chan, R-curve behavior of in-situ-toughened Al_2O_3:-$CaAl_{12}O_{19}$ ceramic composites, Journal of the American Ceramic Society 79 (12) (1996) 3142–3148.
[11] C.J. Russo, M.P. Harmer, H.M. Chan, G.A. Miller, Design of a laminated ceramic composite for improved strength and toughness, Journal of the American Ceramic Society 75 (12) (1992) 3396–3400.
[12] P.E.D. Morgan, D.B. Marshall, Ceramic composites of monazite and alumina, Journal of the American Ceramic Society 78 (6) (1995) 1553–1563.
[13] L. An, H.M. Chan, N.P. Padture, B.R. Lawn, Damage-resistant alumina-based layer composites, Journal of Materials Research 11 (1) (1996) 204–210.
[14] M. Jayasankar, K.P. Hima, S. Ananthakumar, P. Mukundan, P. Krishna Pillai, K.G.K. Warrier, Role of particle size of alumina on the formation of aluminum titanate as well as on sintering and microstructure development in sol–gel alumina–aluminum titanate composites, Materials Chemistry and Physics 124 (2010) 92–96.
[15] R. Uribe, C. Baudin, Influence of a dispersion of aluminum titanate particles of controlled size on the thermal shock resistance of alumina, Journal of the American Ceramic Society 86 (2003) 846–850.
[16] S.Y. Park, S.W. Jung, Y.B. Chung, The effect of starting powder on the microstructure development of alumina–aluminum titanate composites, Ceramics International 29 (2003) 707–712.
[17] S. Bueno, M.G. Hernández, T. Sánchez, J.J. Anaya, C. Baudín, Non-destructive characterisation of alumina/aluminum titanate composites using a micromechanical model and ultrasonic determinations, Part I: evaluation of the effective elastic constants of aluminum titanate, Ceramics International 34 (2008) 181–188.
[18] M.I. Nieto, C. Baudín, I. Santacruz, Reaction sintering of colloidal processed mixtures of sub-micrometric alumina and nano-titania, Ceramics International 37 (2011) 1085–1092.
[19] ASTM C1327-96, 2003. Standard Test Method for Vicker's Indentation Hardness of Advanced Ceramics. Annual Book of ASTM Standards, vol. 15.01.
[20] J.F. Porter, Y.G. Li, C.K. Chan, The effect of calcination on the microstructural characteristics and photoreactivity of Degussa P-25 TiO_2, Journal Of Materials Science 34 (1999) 1523–1531.
[21] P. Bowen, C. Carry, From powders to sintered pieces: forming, transformations and sintering of nanostructured ceramic oxides, Powder Technology 128 (2002) 248–255.
[22] W.F.M. Groot Zevert, A.J.A. Winnubst, G.S.A.M. Theunissen, A.J. Burggraaf, Powder preparation and compaction behavior of fine-grained YTZP, Journal of Materials Science 25 (1990) 3449–3455.
[23] A.A. Bukaemskiy, D. Barrier, G. Modolo, Journal of the European Ceramic Society 29 (2009) 1947–1954.
[24] M. Mazaheri, A.M. Zahedi, M. Haghighatzadeh, S.K. Sadrnezhaad, Sintering of titania nanoceramic: densification and grain growth, Ceramics International 35 (2009) 685–691.